Multi-Functional Self-Healing Polyurethane Elastomer Based on Chair Conformation for Strain Sensors

Yiyao Zhu[a,1], Yuting He[b,1], Wentong Lu[a], Hao Tian[a], Fan Fei[a], Peilong Zhou[a], Jincheng Wang[a]*

a) Department of Polymer Materials and Engineering, College of Chemistry and Chemical Engineering, Shanghai University of Engineering Science, Shanghai 201620, People's Republic of China. Correspondence to: Jincheng Wang (E-mail: wjc406@sues.edu.cn)

b) Department of Geriatrics, Zhongshan Hospital, Fudan University, 180 Fenglin Road, Shanghai 200032, China

#Yiyao Zhu and Yuting He contributed equally to this manuscript.

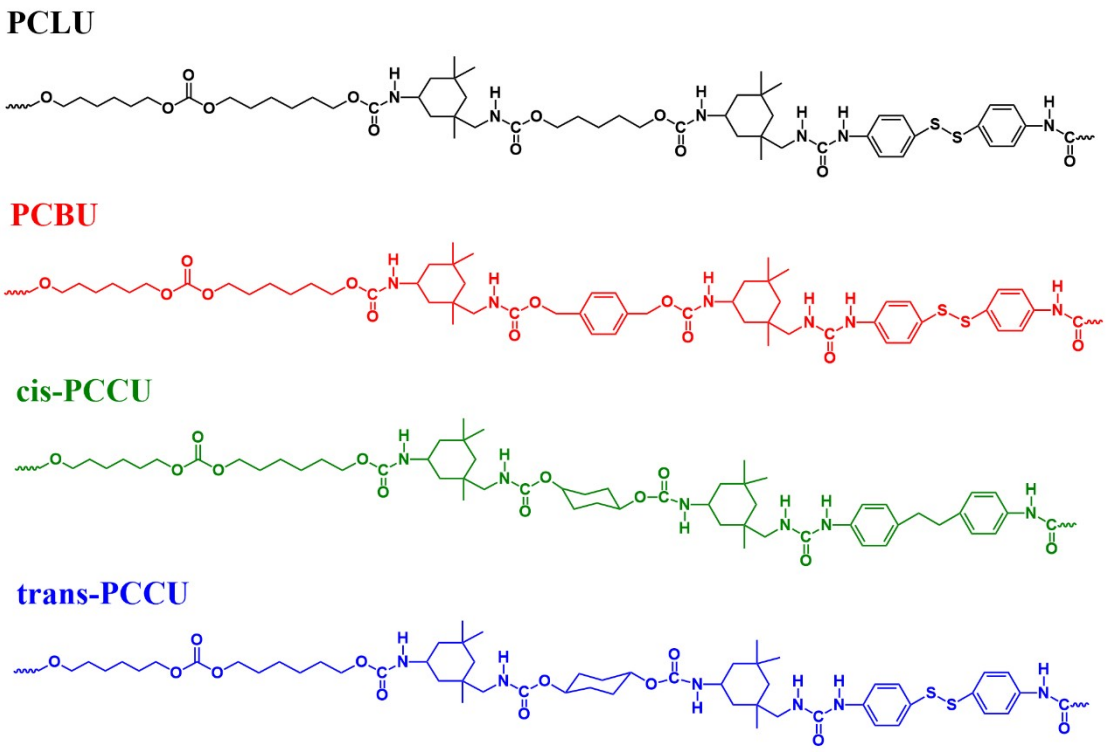

Fig. S1 Chemical structural formulae of PCLU, PCBU, cis-PCCU and trans-PCCU.

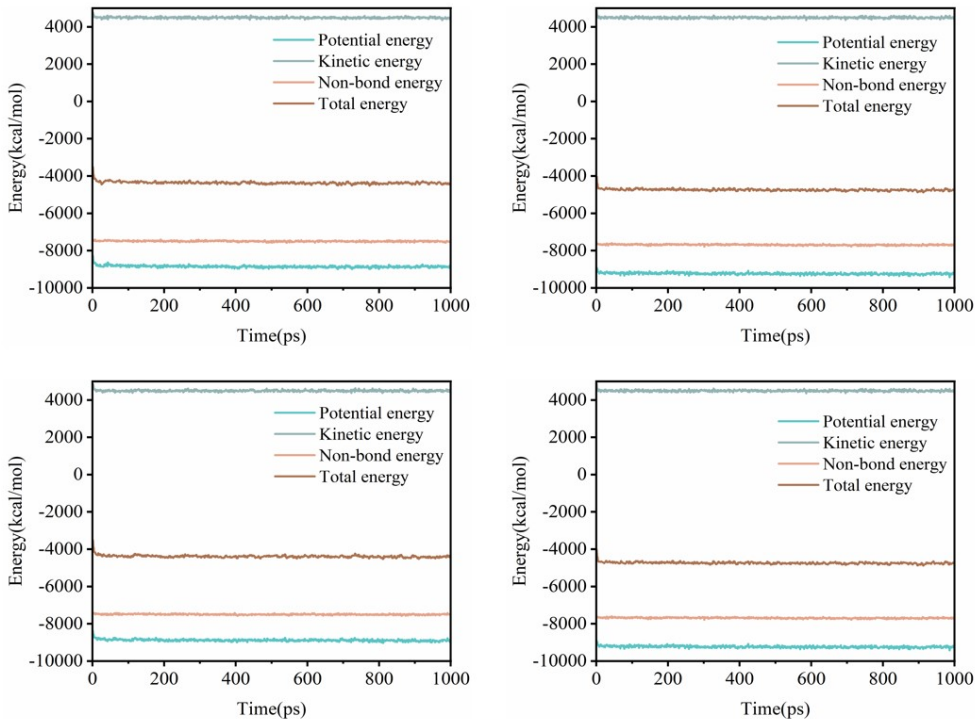

Fig.S2 Statistics on the number of hydrogen bonds, hydrogen bond length and hydrogen bond angle of PCLU, PCBU, cis-PCCU and trans-PCCU.

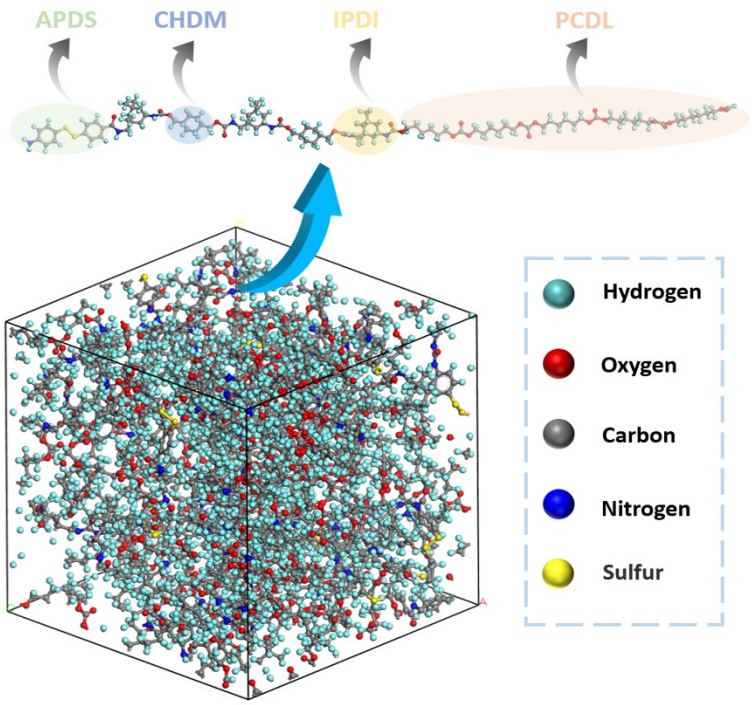

Fig. S3 Single chain model and condensed state model for PCUU system.

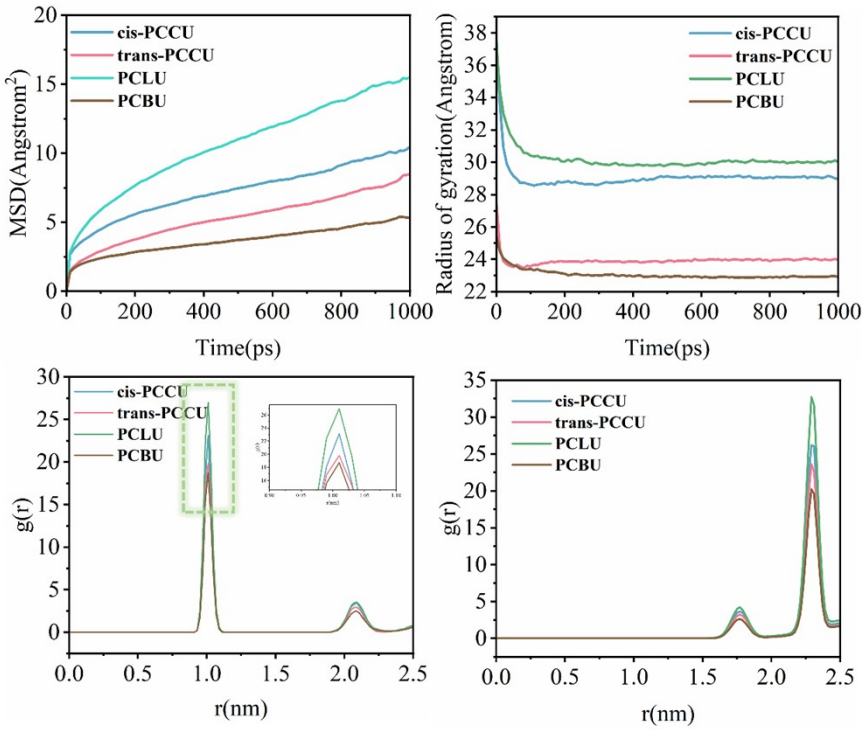

Fig. S4 Mean Square Displacement Functions in Different Systems (i), mean square radius of gyration for different systems(ii), plot of the radial distribution function of the hydrogen bonds formed between N-H(iii) and O-H(iv).

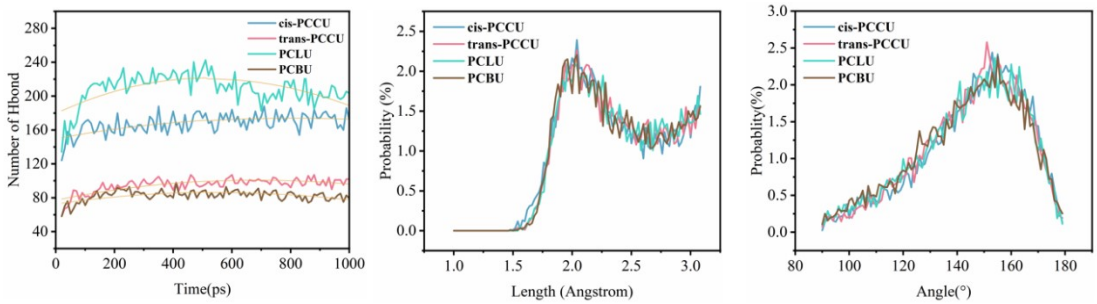

Fig.S5 Energy balance of molecular simulation models for PCLU, PCBU, cis-PCCU and trans-PCCU.

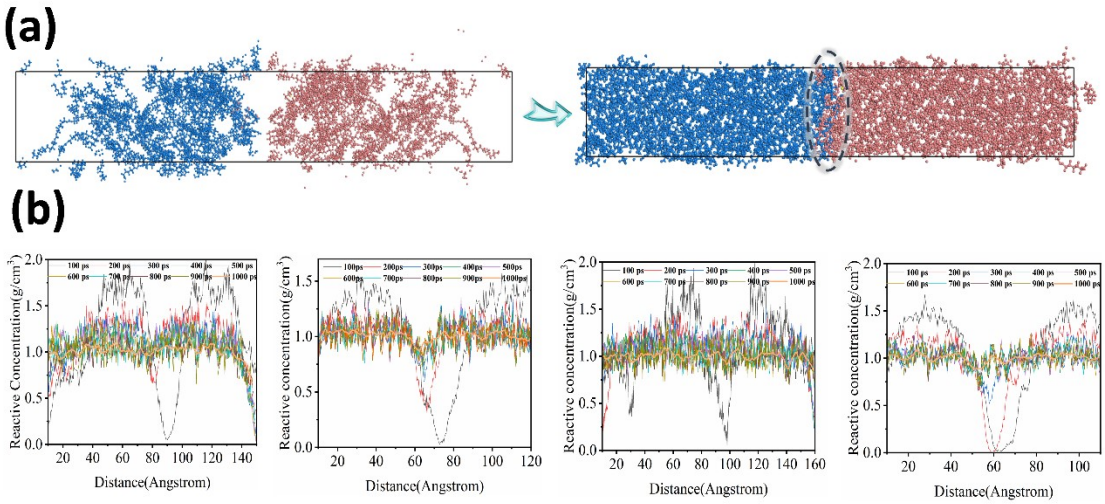

Fig. S6 (a)MD simulates material self-healing processes; (b)Density plots over time for different systems.

Table S1. Molar ratios of raw materials for the synthesis of PCCU-1, PCCU-2 and PCCU-3.

	PCDL-diol	IPDI	CHDM	APDS
PCCU-1	1	3	1	1
PCCU-2	1	4	2	1
PCCU-3	1	5	3	1

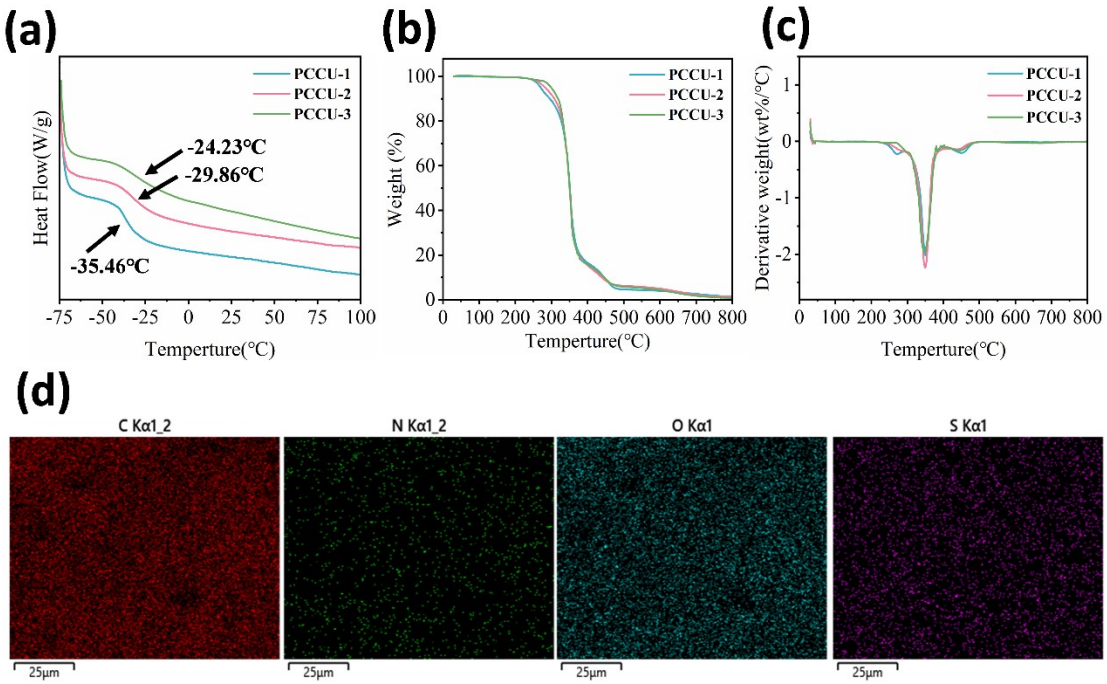

Fig. S7 (a)DSC curves demonstrating the glass transition temperature of PCCU; (b)Heat loss curve of PCCU; (c) DTG curve of PCCU; (d) Distribution of elements in PCCU-2.

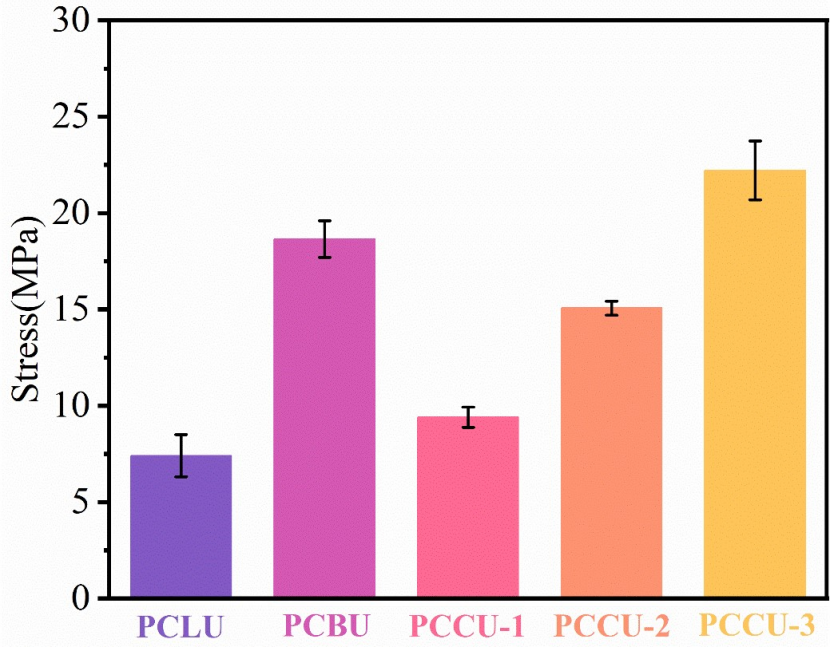

Fig. S8 Statistics of tensile strength of PCLU, PCBU, PCCU-1, PCCU-2 and PCCU-3.

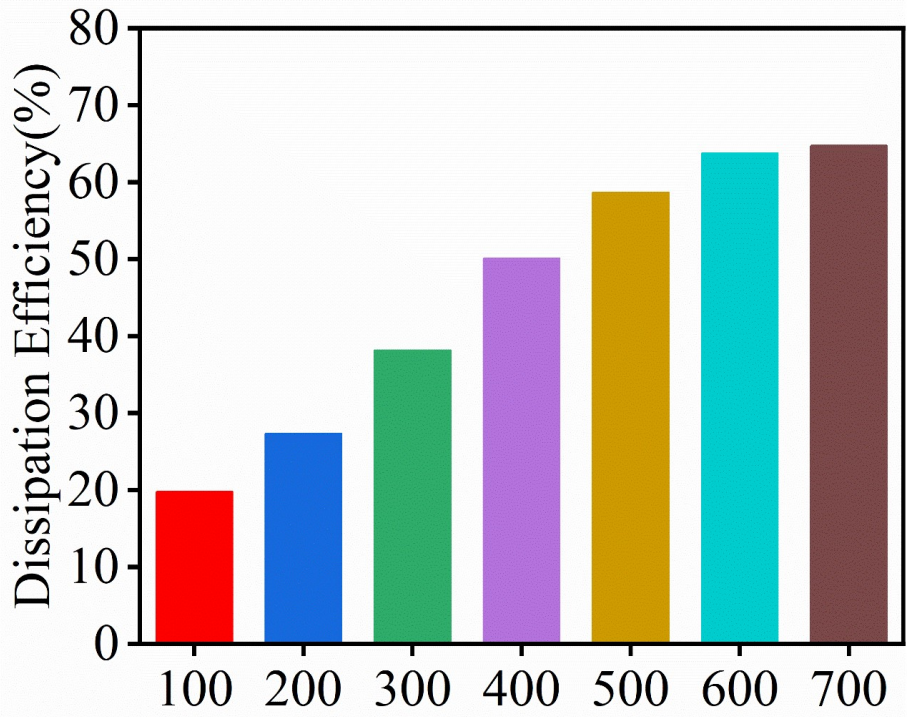

Fig.S9 The statistical graph of the dissipation coefficient of PCCU-2 under tensile cycles at different strains.

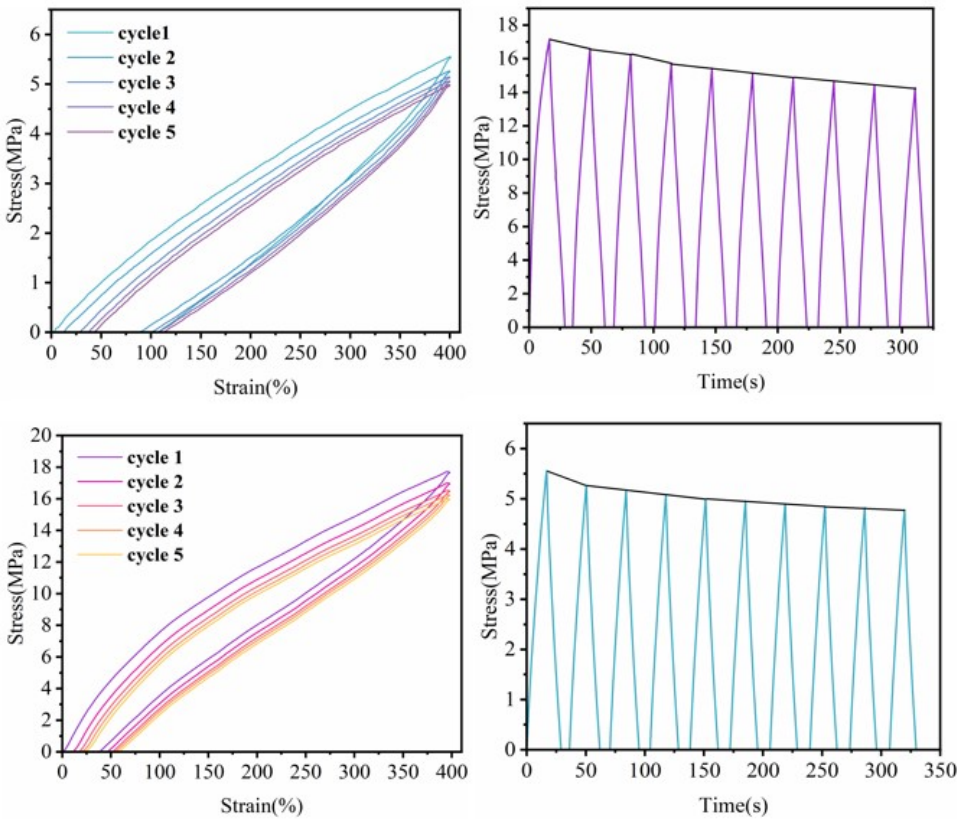

Fig. S10 Tensile cycle curves and stress residual ratio of PCCU-1 and PCCU-3.

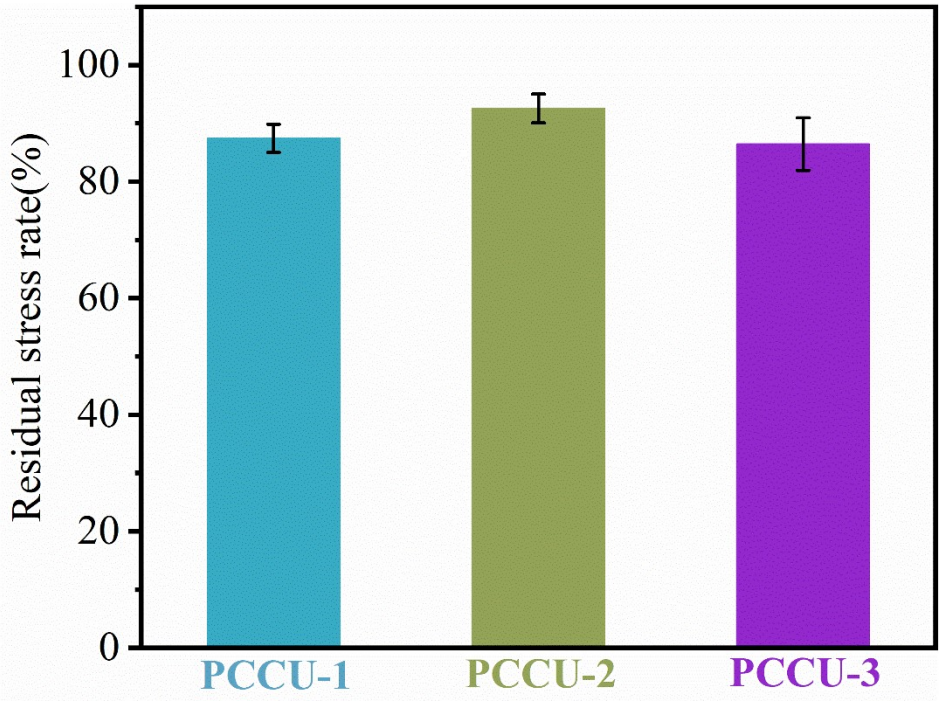

Fig. S11 Statistics on stress residual ratio of PCCU-1, PCCU-2 and PCCU-3.

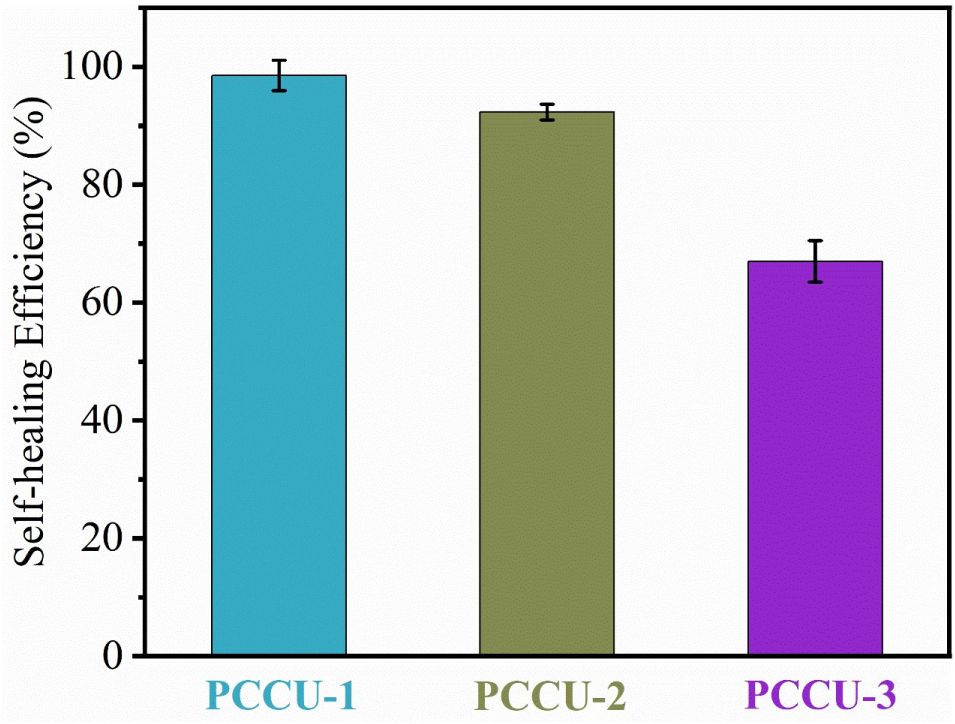

Fig. S12 Statistics on the self-repair efficiency of PCCU-1, PCCU-2 and PCCU-3.

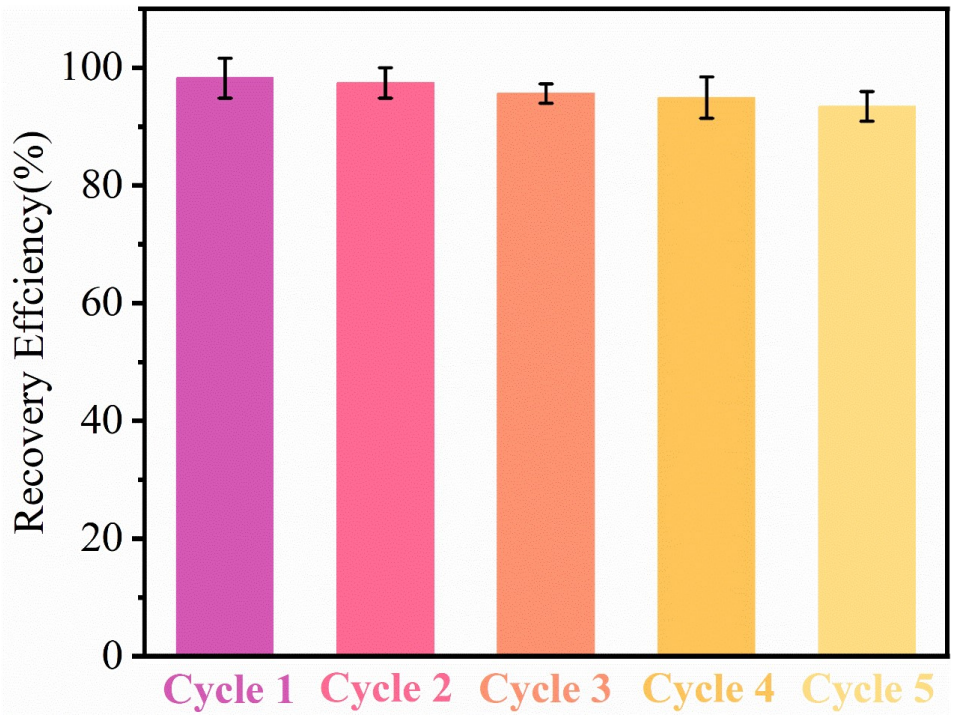

Fig. S13 Statistics on PCCU-2 recycle efficiency after different times in THF.

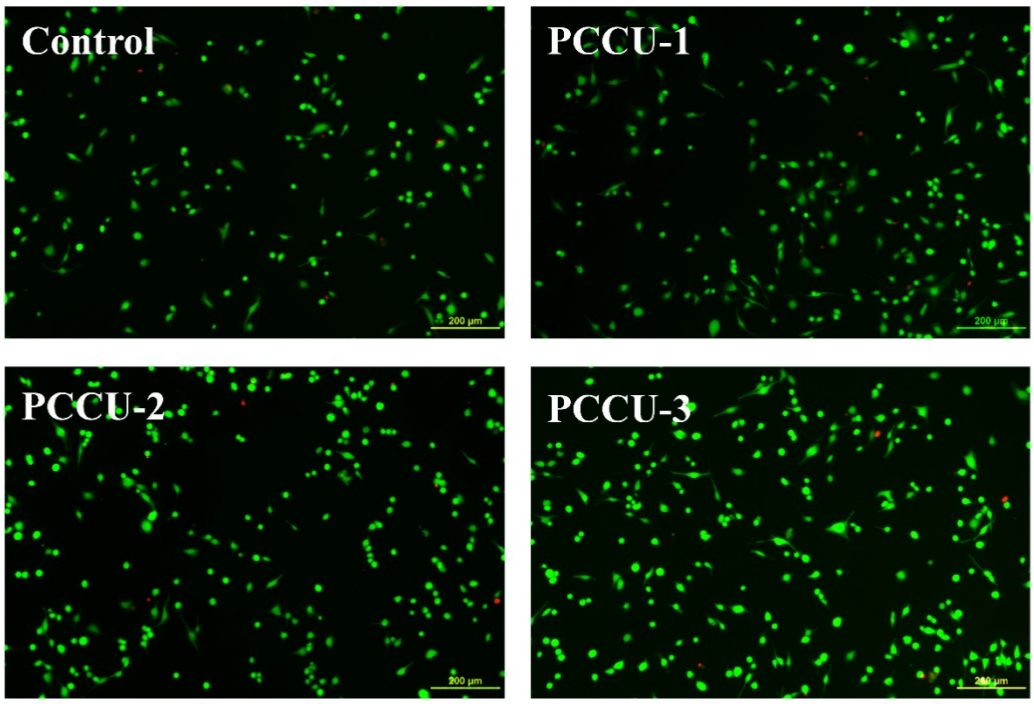

Fig. S14 The microscopic enlargement diagram of spindle formation by fibroblast cells is shown.

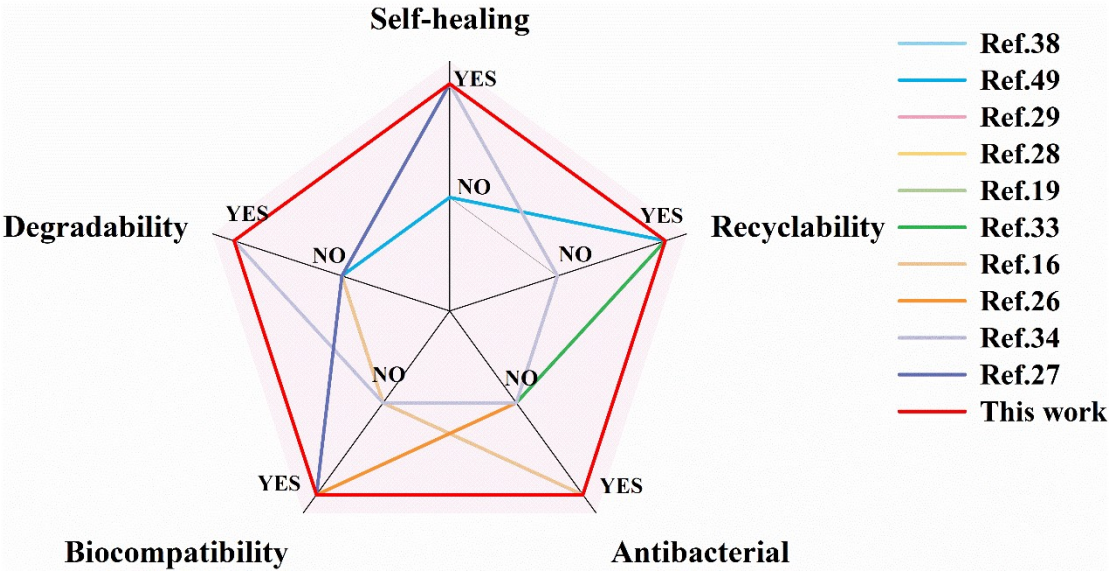

Fig.S15 Scatter plots show a qualitative comparison of this work with other reported sensor studies in terms of five key properties: self-healing, recyclability, degradability, antimicrobial and biocompatibility.

Table S2. This work compares with other reported sensor studies in four performance metrics: tensile strength, elongation at break, self-healing ability, and fatigue resistance.

	Strength (MPa)	Elongation (%)	Self-healing (%)	Biocompatibility (%)	Antibacterial (%)	Recyclability (%)	Degradability (%)
This work	15.09	910	92.75	89.74	92.34	95.04	23.91
Ref.20	0.78	438	76.1	No	No	No	No
Ref.31	14.45	475	95	No	No	Yes	No
Ref.27	1.41	573	99.2	No	Yes	No	No
Ref.36	32	527	No	No	No	85.21	No
Ref.44	34	2014	83	No	No	94.43	No
Ref.38	8.11	983	73	No	No	Yes	No
Ref.49	34.4	1183	No	No	Yes	No	100
Ref.29	43	461	74	Yes	No	Yes	No
Ref.28	39.9	1930	94.4	88	98.63	No	No
Ref.19	75.8	712	88	No	No	Yes	No
Ref.33	29	500	100	No	No	Yes	No
Ref.16	-	-	No	No	No	No	21%
Ref.26	15.99	124	51.6	No	No	No	No
Ref.34	14.08	974	81	No	No	Yes	No

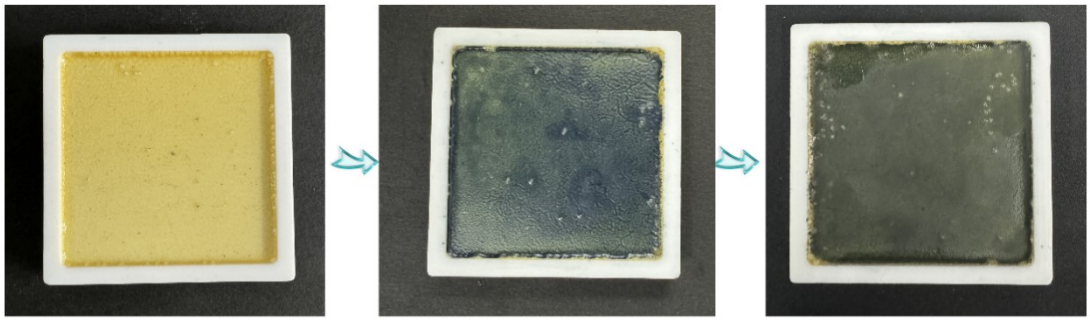

Fig. S16 Flowchart for the preparation of sandwich-structured sensing material.

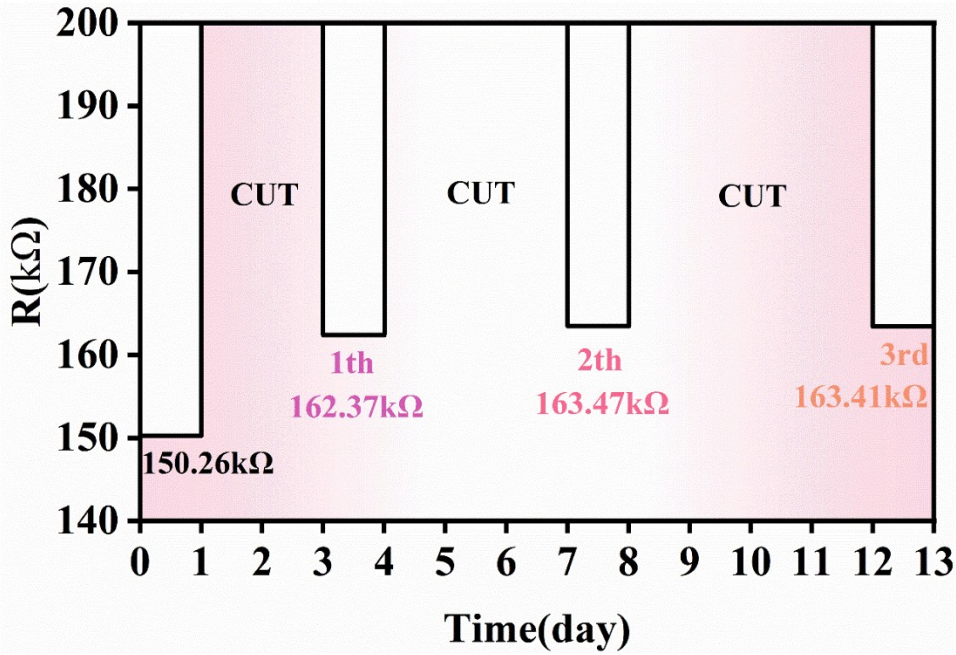

Fig. S17 Long-term stability test of the resistance of PCCU-2 conductive films.

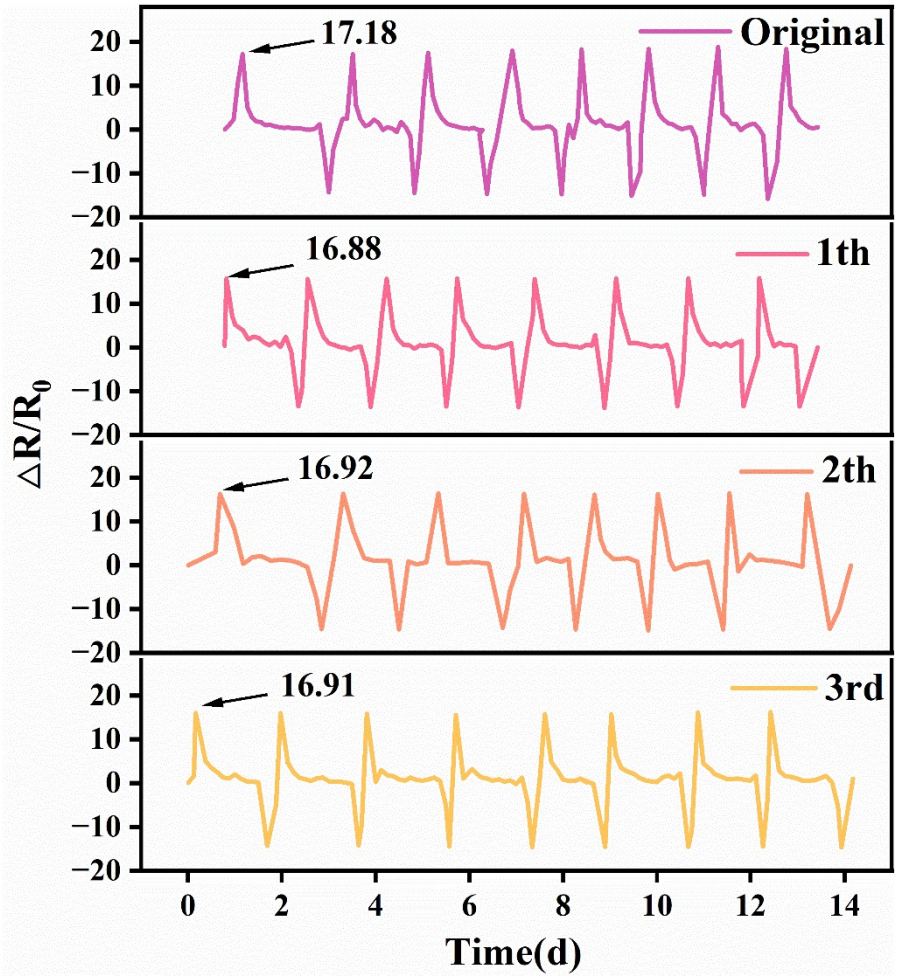

Fig. S18 PCCU-2 conductive film records knee bending signals.

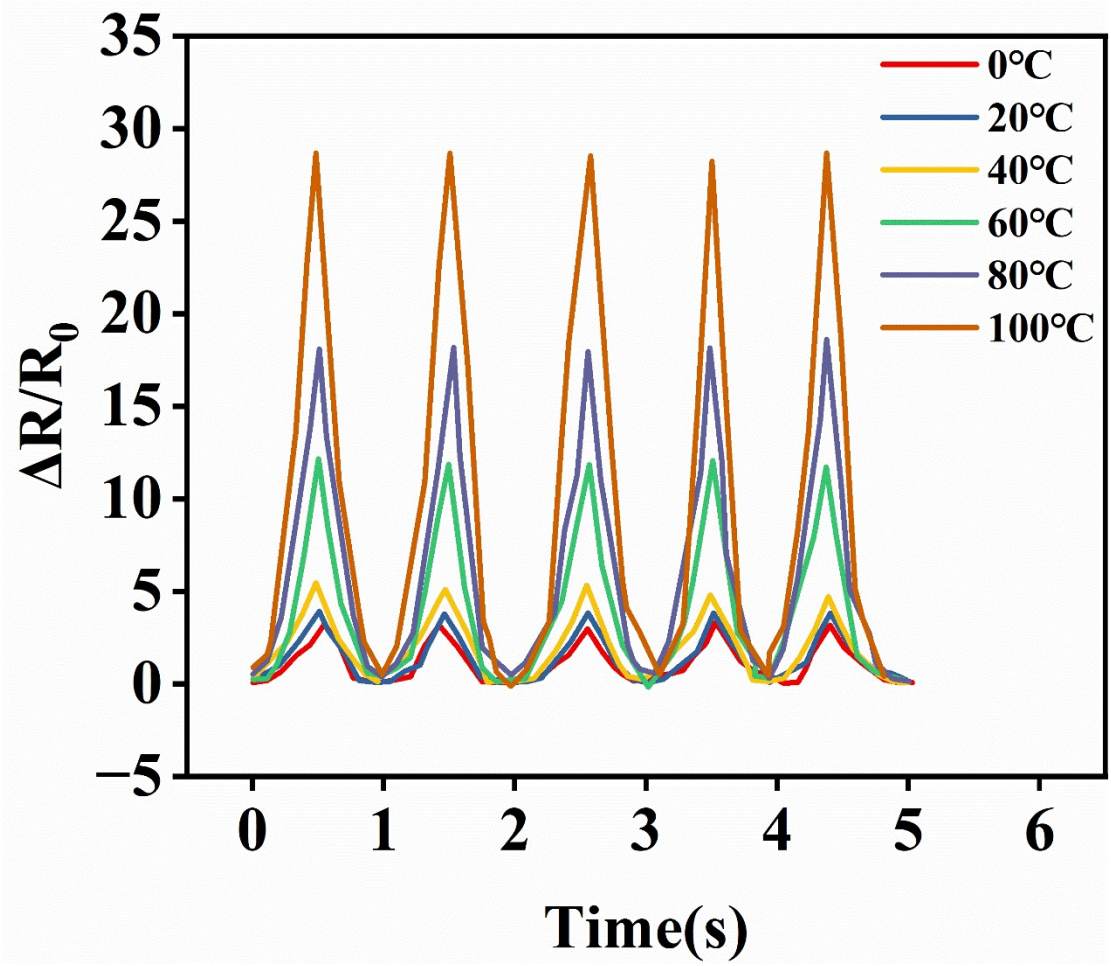

Fig. S19 Signals at different temperatures (50% tensile strain).